




Research Article

LYAR Promotes Colorectal Cancer Progression by Upregulating *FSCN1* Expression and Fatty Acid Metabolism

Yupeng Wu ¹, Yu Zhou,² Haiying Gao,³ Yajun Wang,¹ Qingyu Cheng,⁴ Shikun Jian,⁴ Qi Ding,⁵ Wei Gu,¹ Yanxue Yao,⁵ Jia Ma,¹ Wenjuan Wu,¹ Yuyun Li,¹ Xuhui Tong,⁵ Xiaoyuan Song ⁴ and Sai Ma ²

¹Department of Biochemistry and Molecular Biology, School of Laboratory Medicine, Bengbu Medical College, Bengbu, Anhui 233030, China

²Department of Laboratory, The Affiliated Suzhou Hospital of Nanjing Medical University, Suzhou Municipal Hospital, Gusu School, Nanjing Medical University, Suzhou, Jiangsu 215000, China

³School of Chemistry and Materials Science, University of Science and Technology of China, Hefei, Anhui 230026, China

⁴MOE Key Laboratory for Membraneless Organelles and Cellular Dynamics, Hefei National Laboratory for Physical Sciences at the Microscale, CAS Key Laboratory of Brain Function and Disease, School of Life Sciences, Division of Life Sciences and Medicine, University of Science and Technology of China, Hefei, Anhui 230027, China

⁵School of Pharmacy, Bengbu Medical College, Bengbu, Anhui 233030, China

Correspondence should be addressed to Yupeng Wu; wuyupeng@bbmc.edu.cn, Xiaoyuan Song; songxy5@ustc.edu.cn, and Sai Ma; marseillems@outlook.com

Yupeng Wu, Yu Zhou, and Haiying Gao contributed equally to this work.

Received 16 July 2021; Revised 5 November 2021; Accepted 12 November 2021; Published 6 December 2021

Academic Editor: Alessandro Poggi

Copyright © 2021 Yupeng Wu et al. This is an open access article distributed under the Creative Commons Attribution License, which permits unrestricted use, distribution, and reproduction in any medium, provided the original work is properly cited.

Colorectal cancer (CRC) is a highly malignant tumor associated with poor prognosis, yet the molecular mechanisms are not fully understood. In this study, we showed that LYAR, a nucleolar protein, is expressed at a higher level in CRC tissue than in adjacent normal tissue and that LYAR expression is closely associated with distant CRC metastasis. LYAR not only significantly promotes the migration and invasion of CRC cells *in vitro*, but knockdown (KD) of LYAR in CRC cells also inhibits xenograft tumor metastasis *in vivo*. Microarray analysis of LYAR KD cells combined with a chromatin immunoprecipitation (ChIP) assay, gene reporter assay, and rescue experiment indicated that *FSCN1* (encoding fascin actin-bundling protein 1 (Fascin-1)) serves as a novel key regulator of LYAR-promoted migration and invasion of CRC cells. Knockdown of *FSCN1* significantly inhibits subcutaneous tumorigenesis of CRC cells and leads to the downregulation of *FASN* and *SCD*, genes encoding key enzymes in fatty acid synthesis. In summary, this study reveals a novel mechanism by which LYAR promotes tumor cell migration and invasion by upregulating *FSCN1* expression and affecting fatty acid metabolism in CRC.

1. Introduction

Colorectal cancer (CRC) is the third most frequently diagnosed cancer, with 1.85 million new cases in 2018, and is the second most common cause of cancer-related mortality worldwide [IARC World Cancer Report 2020] [1]. With advances such as prognostic techniques, neoadjuvant chemoradiotherapy, cytotoxic therapy, and surgical therapy, great progress in treat-

ment has been made. The five-year survival rate for CRC, however, remains poor (~64%), and in metastatic cases, it is even worse (14%) [2, 3]. Twenty-five percent of patients with CRC already have metastases at the time of diagnosis, and 50–60% of the remainder will develop metastases later in the course of the disease [4, 5]. The formation of metastasis is a multistep process, in which tumor cells leave the primary tumor site, invade and penetrate the surrounding extracellular matrix

and endothelium, enter the blood and lymph vessels, survive migration, and finally attach at a distant site, where tumor cells begin to proliferate, induce angiogenesis, evade apoptotic death, and form a new tumor [6, 7]. These distant settlements of tumor cells, metastases, are the cause of 90% of human cancer deaths [6, 8–10]. Tumor recurrence and metastasis are the main causes of death in CRC. Approximately 30–50% of patients with CRC after curative surgery will relapse [11]. However, the molecular mechanism involved in the cascade of events during invasion and metastasis of CRC is still not fully understood.

LYAR was first identified in 1993 as a novel nucleolar oncoprotein, which consists of a zinc finger motif and three nuclear localization signals [12]. However, research was stagnant until a second LYAR article was published in 2009 [13]. Subsequently, there have been very few articles related to the function of LYAR [14–18], especially in the field of tumor research. In 2014, Ju et al. demonstrated that LYAR is a transcription factor with a DNA-binding motif (GGTTAT/G) that inhibits human fetal *globin* gene expression [19]. We further reported that LYAR promotes tumor cell migration and invasion by directly binding to the LYAR-binding motif (CTAACC; reverse complement GGTTAG) in the *LGALS1* promoter to activate its expression in CRC cells [20]. *LGALS1* encodes galectin-1, which is a member of the lectin family. Galectin-1 is a homodimer of 14 kD subunits and is characterized by its affinity for glycans containing β -galactosides. Galectin-1 has been detected in various malignancies such as colorectal, hepatocellular, prostate, ovarian, and breast cancers. Galectin-1 activation occurs via autocrine or paracrine sugar-dependent interactions with β -galactoside-containing glycoconjugates and participates in various key processes of carcinogenesis such as metastasis, angiogenesis, and immunosuppression [21].

The *FSCN1* gene is located on chromosome 7p22 and encodes Fascin-1, a cytoskeleton protein with a relative molecular weight of 55 kD [22]. Fascin-1 can promote the formation of filamentous pseudopodia, lamellar pseudopodia, and microspines of cell membrane after cross-linking with F-actin. This enhances the movement, metastasis, and invasion of tumor cells [23]. A mass spectrometry-based proteomic analysis predicted that *FSCN1* may play an important role in metabolism, suggesting a new role of *FSCN1* in tumors [24].

In the present study, we showed that LYAR, a key regulator of CRC, regulates a novel LYAR target, *FSCN1*, to promote the migration and invasion of CRC cells, which in turn positively regulates fatty acid metabolism. Our data demonstrated the presence of a LYAR/*FSCN1*/fatty acid metabolism axis which promoted the growth of CRC tumors *in vivo*. These findings suggest that LYAR could be used as a prognostic and therapeutic candidate target for the prevention and treatment of CRC.

2. Materials and Methods

2.1. Tissue Microarrays and Immunohistochemistry. CRC tissue arrays were purchased from Shanghai Outdo Biotech Co., Ltd., Shanghai, China. The immunohistochemistry exper-

iment and analysis were carried out according to the procedure described in our previous literature [20]. The LYAR primary antibody (orb215217) and the anti-rabbit secondary antibody were purchased, respectively, from Biorbyt and Sigma-Aldrich. All researches involving human CRC tissues were approved by the Ethics Committee of Bengbu Medical College and were in accordance with the principles of the Declaration of Helsinki.

2.2. Cell Lines and Cell Culture. The HCT8, HCT15, and HCT116 human colon cancer cell lines were purchased from the Typical Culture Preservation Commission Cell Bank, Chinese Academy of Sciences. HCT8 and HCT15 was maintained on gelatinized 10 cm-plate in RPMI-1640 Medium (Gibco) supplemented with 10% FBS (fetal bovine serum) (Gibco), 100 U penicillin/100 mg streptomycin (Gibco) at 37°C, and 5% CO₂. HCT116 cells were cultured in McCoy's 5a Medium (Gibco).

2.3. Silencing of LYAR and FSCN1 by Transient Transfection siRNA. The siRNA sequences against human LYAR, *FSCN1* and nonsilencing were designed and chemically synthesized by Genepharma (Shanghai, China). HCT15 cells were transfected with 100–200 pmol siRNA using 5–10 μ L INTERFERin® transfection reagent (Polyplus) in a 6-well plate. After 24–48 hours, cells were collected to perform cell proliferation, cell cycle, apoptosis, colony formation, adhesion, migration, and invasion assays. The siRNAs sequences were as follows:

- (1) Human LYAR-siRNA1: 5'-GGGAGGUGAAGAAG AAUAA-3'
- (2) Human LYAR-siRNA2: 5'-GCACUCGGAAGUUG AAACA-3'
- (3) Human FSCN1-siRNA1: 5'-GCGCCUACAACAUC AAAGA-3'
- (4) Human FSCN1-siRNA2: 5'-GCCCAUGAUAGUAG CUUCA-3'

2.4. Microarray Analysis and RNA-Seq. Approximately 1 \times 10⁷ cells were collected and lysed with TRIzol® Reagent (Life Technologies) in the RNase-free Eppendorf tube. We then submitted the samples to KangChen-Biotech Corporation (Shanghai, China) for microarray analysis using the Human 12 \times 135K Gene Expression Array (Roche NimbleGen). The experiment and data analysis for microarray analysis, including RNA isolation, microarray experiment, data processing, statistical analysis, and gene ontology analysis, were done by KangChen-Biotech Corporation.

FSCN1 siRNA and NC (negative control) were transfected into cells and cultured for 24–48 hours. Then, total RNA was isolated by the RNA pure Tissue and Cell Kit and the RNA was sequencing by the 150 bp paired method. Hisat2, samtools, and htseq-count packages were used to align 150 bp paired-end reads with hg19 (UCSC). The expression of genes and transcripts was quantified by using cufflinks tools.

We downloaded expression profiles of human colorectal cancer of TCGA and normal colon data of GTEx from UCSC Xena browser (<https://xenabrowser.net/datapages/>).

2.5. Plasmid Construction and Viral Infection. To build stable knockdown cells, the small hairpin RNAs (*LYAR*-shRNAs, *FSCN1*-shRNAs, and Control-shRNA) were designed correspondingly according to the sense and antisense sequences of the two *LYAR*-specific siRNAs and *FSCN1* siRNAs (see above) and a nonspecific siRNA and synthesized by Invitrogen (Shanghai, China). These chemically synthesized oligonucleotides were annealed to generate double-stranded oligonucleotides using the touchdown program in the PCR instrument and inserted into the *Xho* I/*Hpa* I sites in the pLentiLox 3.7 vectors, which was subsequently confirmed by sequencing.

To overexpress *FSCN1*, the human *FSCN1* coding sequence (CDS) was prepared by reverse transcription-polymerase chain reaction (RT-PCR) from normal colorectal tissues and cloned into the pLVX-IRES-mCherry Vector at *Xba* I and *Bam*H I sites for overexpressing *FSCN1* in *LYAR*-KD cells. Lentiviruses were packaged and produced in 293T cells. The supernatant of virus production was collected and filter-sterilized to infect the corresponding cells. The stably transfected cells were sorted and collected by flow cytometry using mCherry fluorescence.

2.6. Cell Migration and Invasion Assays. Equal amounts of cells (1×10^5 in 200 μ L medium without FBS) were seeded on a fibronectin-coated polycarbonate membrane insert in a Transwell apparatus (Corning Costar), and medium supplemented with 20% FBS was added to the lower chamber. After incubation for 48 h at 37°C, the insert was washed with phosphate-buffered saline, and cells on the upper surface of the insert were removed by wiping with a wet cotton swab. Cells migrating to the lower membrane surface were fixed by an equal volume mixture of methanol and acetone and stained with 0.4% crystal violet and counted under a microscope (Nikon). The invasion assay was executed as described in the migration assay using upper chamber pre-coated with 50 μ L matrigel solution that original matrigel (BD Biosciences) was diluted with FBS-free medium according to the ratio of 1:10.

2.7. Quantitative RT-PCR (RT-qPCR). Total RNA was isolated from cells with TRIzol® Reagent (Life Technologies). cDNA was synthesized using HiScript® II 1st Strand cDNA Synthesis Kit (+gDNA wiper) (Vazyme). The RT-qPCR primers were designed by Primer Premier 6.0 software. RT-qPCR was carried out in a Rotorgene 6000 (Corbett Research) using the FastStart Universal SYBR Green Master Mix (Roche) in a final volume of 20 μ L. The relative quantification was executed for the following genes using *GAPDH* as an internal reference in CRC cells. Each reaction was performed in triplicate and repeated at least two times.

The primers for human *GAPDH* were as follows:

- (1) Forward 5'-ACCATCTTCCAGGAGCGAGA-3'
- (2) Reverse 5'-GTTACACCCATGACGAACATG-3'

The primers for human *LYAR* were as follows:

- (1) Forward 5'-GGAGGCACTCGGAAGTTGAAA-3'
- (2) Reverse 5'-GTTCTCTTCGGATCTGTGATG-3'

The primers for human *FSCN1* were as follows:

- (1) Forward 5'-CTGCTACTTTGACATCGAGTGG-3'
- (2) Reverse 5'-GGGCGGTTGATGAGCTTCA-3'

The primers for human *FASN* were as follows:

- (1) Forward 5'-GCTGGAAGGAGGAAGAGGTT-3'
- (2) Reverse 5'-CTCGAGTGGTCCGTGAGTTT-3'

The primers for human *SCD* were as follows:

- (1) Forward 5'-CTCAGTTCCTACGCTTCGCAT-3'
- (2) Reverse 5'-GTCGAGGTCAGTGAACAGCA-3'

2.8. Western Blotting. Cell extracts were prepared using the lysis buffer (Beyotime) from the CRC cell lines. Cell lysates (20-50 μ g) were loaded and separated by 10-15% sodium dodecyl sulphate-polyacrylamide gel (Bio-Rad) and transferred onto nitrocellulose membranes (Millipore). After 1 h blocking with 5% nonfat milk (or 3% BSA (bovine serum albumin)) blocking solution prepared with PBST (1 \times PBS with 0.1% Tween-20), the membranes were incubated overnight at 4°C with the primary antibodies against *LYAR* (orb215217, Biorbyt), *FSCN1* (ab220195, Abcam), *FASN* (10624-2-AP, Proteintech), *SCD* (2794S, CST), and *GAPDH* (M171-3, MBL) as the internal control and followed by incubation with the secondary antibody (Sigma-Aldrich) for 1 h at room temperature. The specific bands were visualized with Thermo SuperSignal® West Pico Chemiluminescent Substrate (Thermo Fisher Scientific Inc.).

2.9. Luciferase Reporter Assay. The *FSCN1* promoter region with a 496-bp sequence containing the specific DNA-binding motif for *LYAR* was amplified from the genomic DNA by PCR. Subsequently, the 496-bp DNA fragment product was subcloned into pGL3-Basic (Promega) to construct a luciferase reporter plasmid (pGL3-*FSCN1*-496bp-*LYAR*-wildtype), and the sequence was confirmed by double-direction sequencing (Invitrogen). Based on the pGL3-*FSCN1*-496bp-*LYAR*-wildtype plasmid, the pGL3-*FSCN1*-496bp-*LYAR*-mutant plasmid was constructed using the Muta-direct™ site-directed mutagenesis kit (SBS Genetech) for mutating the *LYAR* binding site. Luciferase reporter assays were performed as described previously [25].

2.10. Chromatin Immunoprecipitation (ChIP). ChIP assays were performed following standard ChIP procedures [26]. Chromatin fractions from HCT15 cells were immunoprecipitated with *LYAR* primary antibody (a kind gift from the State Key Laboratory of Pharmaceutical Biotechnology,

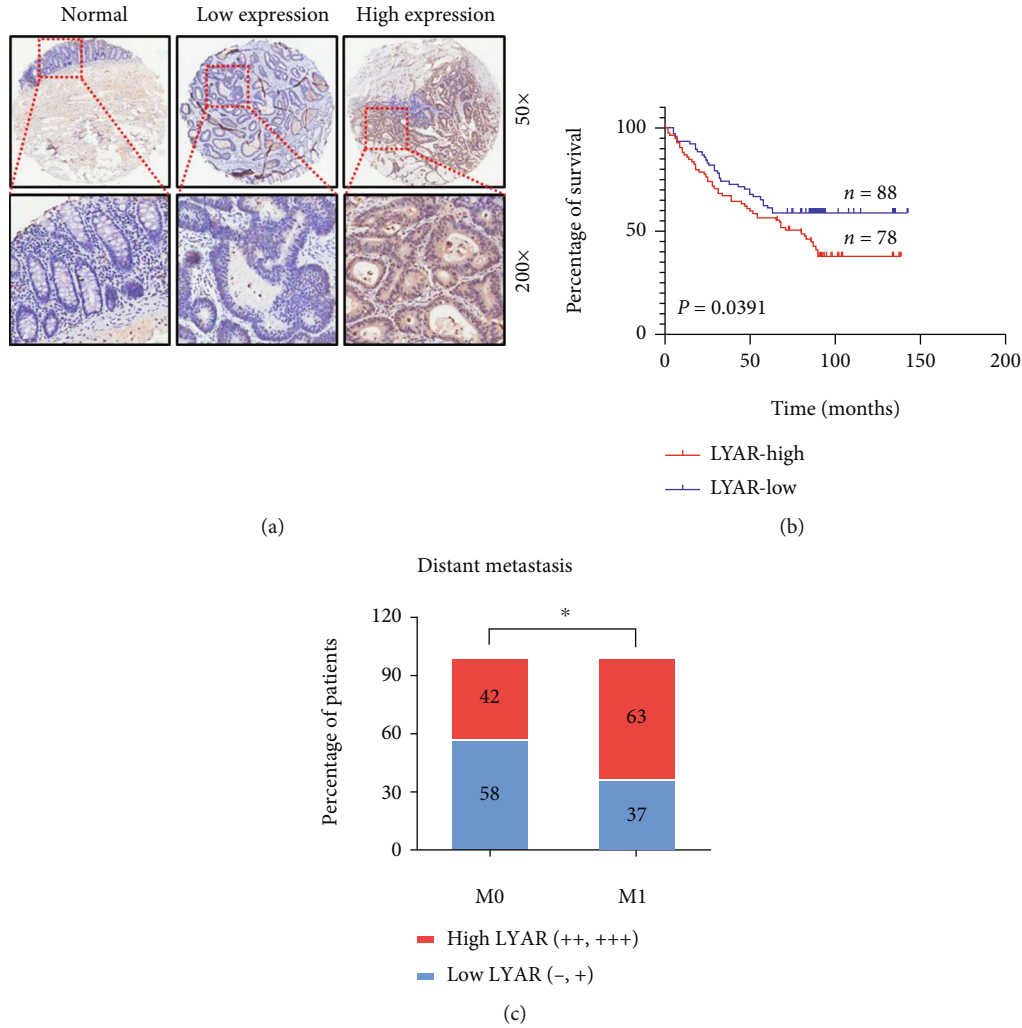


FIGURE 1: LYAR is highly expressed in human CRC tissues. (a) Immunohistochemical staining showing the LYAR protein (brown) in adjacent normal colorectal tissue and carcinoma tissue from CRC patients. Representative micrographs are shown at the original magnification (50x and 200x). Low and high LYAR expressions were defined based on immunostaining scores [20]. (b) The prognostic curve of LYAR. (c) The percentage of patients with different metastasis statuses (M0: no regional or distant metastasis; M1: regional or distant metastasis). * $p < 0.05$.

School of Life Sciences, Nanjing University, Nanjing, China). Normal rabbit immunoglobulin G (IgG, Beyotime) served as the controls. The ChIP samples were analyzed by quantitative real-time PCR using the FastStart Universal SYBR Green Master Mix (Roche) and specific primers (Table S2) spanning the *FSCN1* promoter. A standard curve was prepared for each set of primers using serial titrations of the input DNA. The percentage of ChIP DNA was calculated relative to the input DNA from primer-specific standard curves using the Rotor-Gene 6000 Series Software 1.7. Each experiment was performed at least two independent times.

2.11. Rescue Experiments. The supernatant of virus production of pLVX-IRES-mCherry (empty vector) and pLVX-IRES-mCherry-*FSCN1*-OE (exogenous expression of *FSCN1*) were used, respectively, to infect the stable LYAR-KD and LYAR-Control (only infected by empty vector) cells. Those stably infected cells were sorted and collected using

TABLE 1: LYAR is highly expressed in human CRC tissues.

	Total	Positive (LYAR high expression)	Positive rate	χ^2	p
Adjacent	166	8	4.8%	81.806	<0.001
CRC	166	78	47.0%		

mCherry fluorescence by flow cytometry, followed by cell migration and invasion assays (see above).

2.12. Animal Experiments. Mice were purchased from and housed at Suzhou University. All animal studies were approved by the ethical regulations of Institutional Animal Care and Use Committee (IACUC) of Suzhou University. For the tumor metastasis assay, stable HCT15 clones (Control or LYAR-KD1) were injected into six-week-old female NOD/SCID mice. For each group, 10 mice were injected with 1×10^6 cells per animal via the tail vein. The mice were

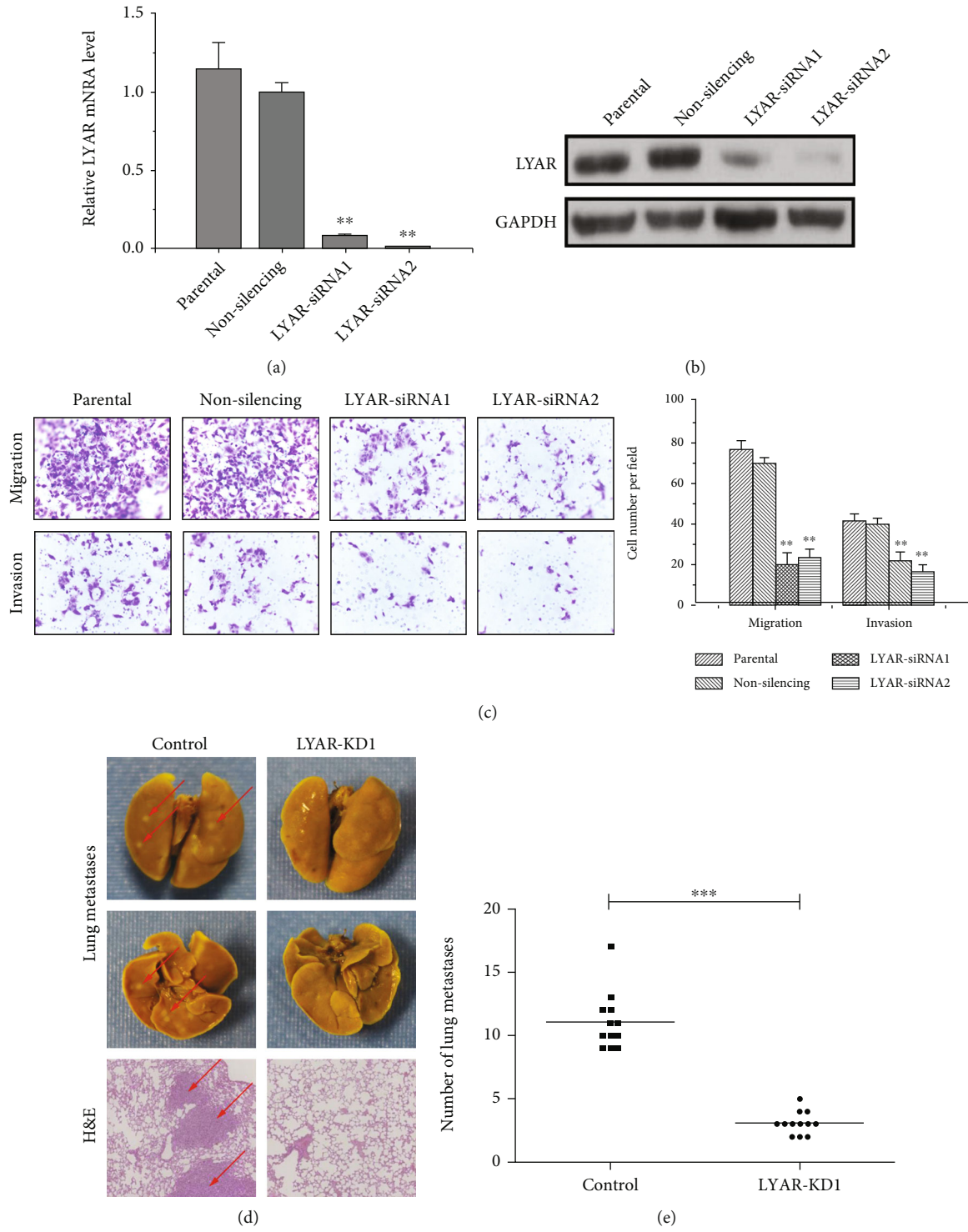


FIGURE 2: Continued.

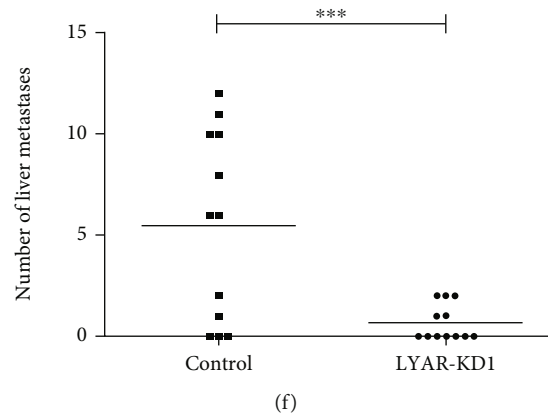


FIGURE 2: LYAR promotes metastasis of CRC cells. (a) Quantitative RT-PCR analysis of *LYAR* expression normalized to *GAPDH* expression in LYAR knockdown HCT15 cells. Results shown are the mean \pm standard deviation ($n = 3$). $**p < 0.01$ compared with the nonspecific siRNA control. (b) Western blot assay showing LYAR protein expression in LYAR knockdown HCT15 cells. GAPDH served as the loading control. (c) At left, representative photos of haptotactic migration assay and matrigel chemoinvasion assay using LYAR knockdown HCT15 cells. Original magnification, 200x. At right, the percentage of migrated and invaded LYAR knockdown HCT15 cells compared to the control. $**p < 0.01$. (d) Representative images of metastatic nodules (indicated with arrows) in lung tissues after Bouin's fixation (upper four panels) and hematoxylin and eosin (H&E) staining of tissue sections (lower two panels). (e) Visible lung metastasis counts. $***p < 0.001$. (f) Visible liver metastasis counts. $**p < 0.01$.

sacrificed 6 weeks after injection, and the lung and liver metastases were examined. Metastatic nodules in lung and liver tissues were fixed in Bouin's solution (Appligen), and the number of metastases was counted. The tumor samples were embedded in paraffin, cut into $5\ \mu\text{m}$ sections, and stained with hematoxylin and eosin (H&E).

For the tumor xenograft assay, 8 six-week-old female nude mice were processed by subcutaneous implantation of 1×10^6 HCT15 cells expressing either control shRNA or *FSCN1*-shRNA. Mice were maintained for 30 days, and tumor volumes were measured at indicated time points. At the end of experiments, mice were euthanized and xenograft tumors were dissected for further analyses.

2.13. Statistical Analysis. All statistical analyses were performed using SPSS 22.0 software (SPSS Inc. Chicago, IL, USA). The experimental results were statistically evaluated using *Student's t-test* for comparisons between two groups or ANOVA for comparisons between more than two groups. Kaplan-Meier survival curves were generated to determine the relationship between *LYAR* levels and the overall survival of CRC patients, and the differences between the curves were calculated using the log-rank test. Multiple Cox proportional hazards regression was carried out to identify the independent factors with a significant impact on patient survival. p values < 0.05 were considered statistically significant.

3. Results

3.1. LYAR Is Highly Expressed in Human CRC Tissue and Promotes CRC Metastasis. Based on data from the OncoPrint database (<https://www.oncoPrint.org/>) and a previous study [20], we found that LYAR was highly expressed and promoted cell mobility in CRC cells. However, the relationship between the high expression level of LYAR and the survival rate of CRC patients is unclear. To answer this

question, we performed immunohistochemistry (IHC) analysis of LYAR on tissue arrays of 166 paraffin-embedded adjacent sections of normal colorectal tissues and CRC tissues. Tissues that displayed moderate or strong immunostaining were classified as having high LYAR expression and those that displayed negative or weak immunostaining as having low LYAR expression. There was strong LYAR staining in only 4.8% (8/166) of the adjacent normal epithelial tissues, whereas $\sim 47.0\%$ (78/166) of total CRC tissues had high expression levels of LYAR (Figure 1(a), Table 1, and Table S1). Furthermore, high LYAR expression was significantly correlated with poor prognosis (Figure 1(b)), which was consistent with the survival curve analysis of CRC data from The Cancer Genome Atlas (TCGA) database (Figure S1). Notably, LYAR expression was positively correlated with a higher metastasis status (Figure 1(c) and Table S1). Taken together, these results indicate that LYAR is highly expressed in CRC tissues, particularly metastatic tissues. This suggests that LYAR may be involved in metastasis of CRC cells, with the potential to be a novel prognostic biomarker for CRC.

LYAR has zinc finger DNA-binding motifs and binds to DNA at the GGTTAT/G consensus sequence [12, 19]. To perform a systematic analysis and to take our previous research a step forward, we verified that LYAR promoted migration and invasion of HCT15 cells *in vitro* (Figures 2(a)–2(c) and Figure S2–4). More importantly, we found that LYAR enhanced the lung and liver metastasis of CRC cells through a mouse tail vein assay *in vivo*. (Figures 2(d)–2(f)).

3.2. FSCN1 Is a Novel Target of LYAR. Heterogeneity is a distinctive feature of solid tumors. Therefore, we speculated that there is more than one molecular mechanism by which LYAR promotes CRC migration and invasion, in addition to upregulating *LGALS1*. In order to comprehensively identify

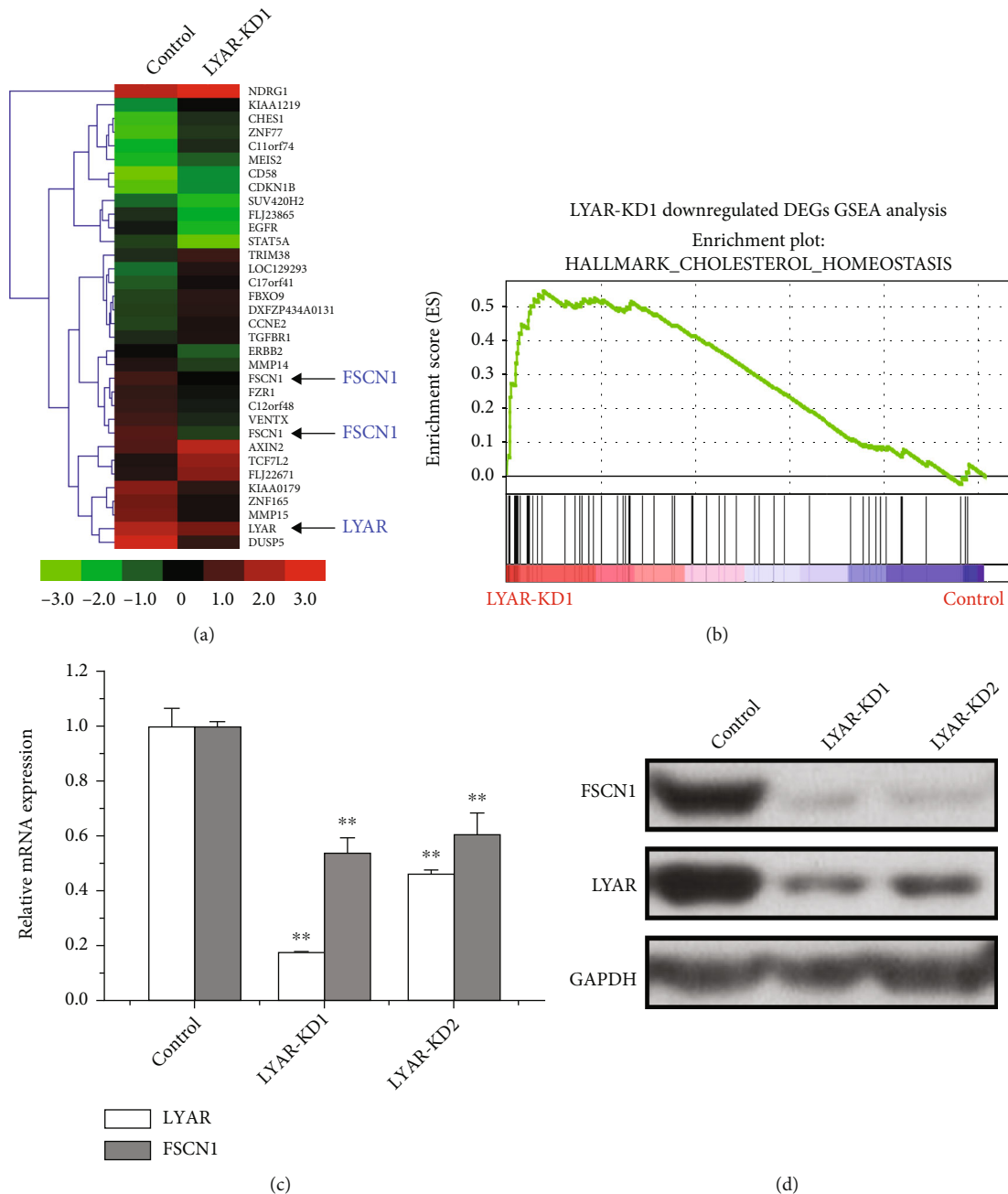


FIGURE 3: *FSCN1* is a novel target of *LYAR*. (a) Heatmap representation of gene expression for *LYAR* and *FSCN1* (indicated with arrows) and selected other genes in the *LYAR* knockdown or control HCT15 cells. Color represents expression values, with green indicating low, black indicating medium, and red indicating high expression. (b) Gene Set Enrichment Analysis (GSEA) plots of RNA-Seq in *LYAR* knockdown HCT15 cells. (c) Quantitative real-time PCR analysis of *LYAR* and *FSCN1* from *LYAR* knockdown or control HCT15 cells. Results shown are the mean \pm standard deviation ($n = 3$). ** $p < 0.01$. (d) Western blot assay showing *LYAR* and *FSCN1* protein expression in *LYAR* knockdown HCT15 cells. GAPDH served as the loading control. KD1 and KD2 refer to stable *LYAR* knockdown lines *LYAR*-siRNA1 and *LYAR*-siRNA2, respectively.

regulatory roles of *LYAR* in metastatic CRC, a whole-genome microarray analysis of gene expression was performed in *LYAR* knockdown (KD) and control HCT15 cells (Figure 3(a)). Gene Set Enrichment Analysis (GSEA) showed that differentially expressed genes (DEGs) in the *LYAR*-KD line were significantly enriched in cholesterol homeostasis, a lipid metabolism-related pathway (Figure 3(b)). We then

screened for genes associated with metastasis and metabolism among the DEGs. The upstream promoter region (2000 bp upstream of the transcription start site) of each candidate gene was searched for the GGTTAT/G motif, which is the consensus DNA-binding site of *LYAR*. Candidate genes with this motif were selected for further analysis in HCT15 cells. Quantitative RT-PCR (RT-qPCR) revealed that the

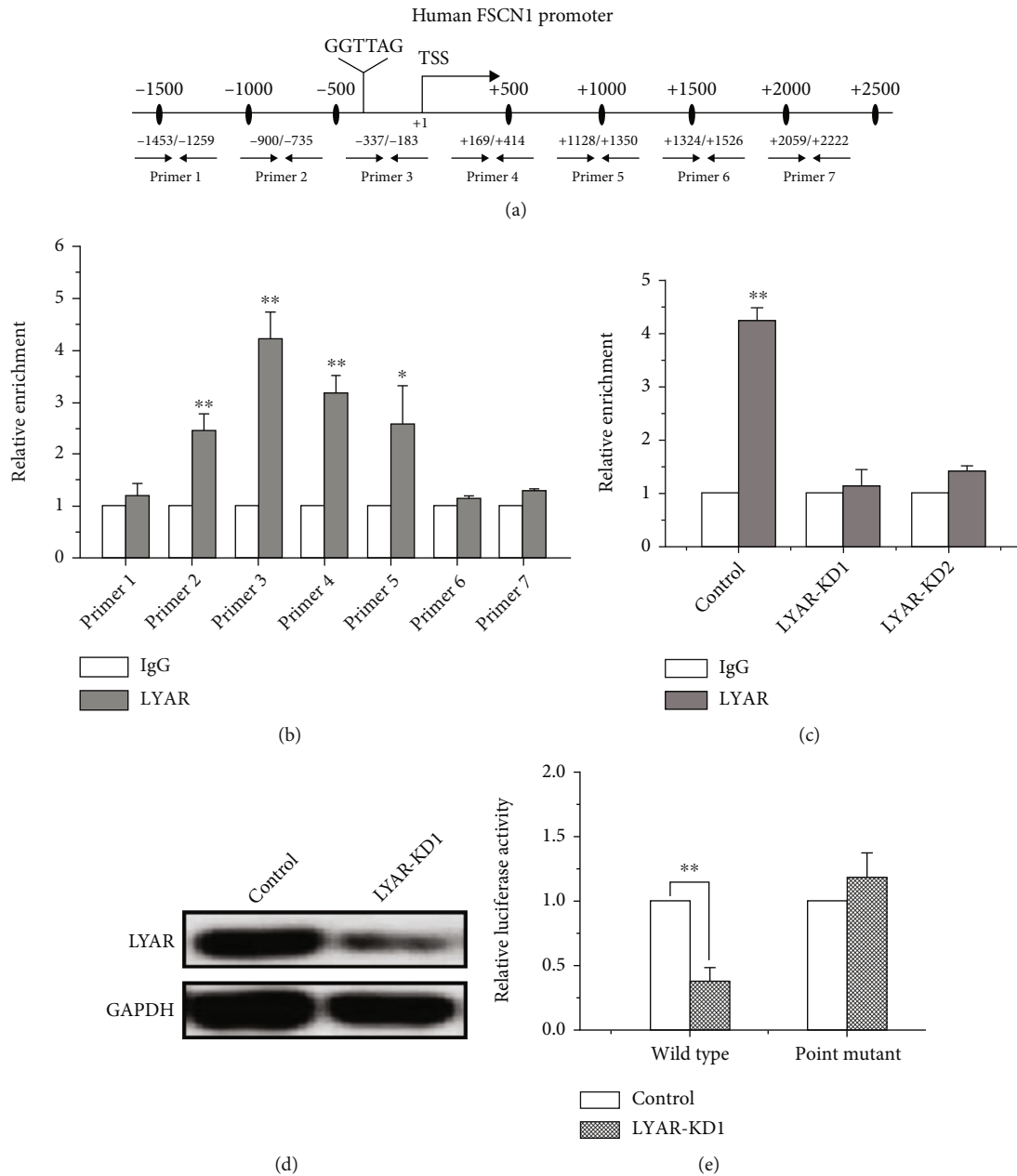


FIGURE 4: LYAR binds to the *FSCN1* promoter and directly activates the expression of *FSCN1*. (a) A schematic diagram showing seven primer pairs spanning the *FSCN1* promoter that were designed for ChIP. (b) ChIP analysis of LYAR on the *FSCN1* promoter in HCT15 cells. Normal rabbit IgG served as the control. Results are shown as the mean \pm standard deviation ($n = 3$). ** $p < 0.01$ and * $p < 0.05$ compared to the IgG control. (c) ChIP analysis of LYAR on the *FSCN1* promoter in LYAR knockdown and control HCT15 cells. Normal rabbit IgG served as the control. Results are shown as the mean \pm standard deviation ($n = 3$). ** $p < 0.01$ compared to the IgG control. (d) Western blot assay showing LYAR protein expression in LYAR knockdown HCT15 cells. GAPDH served as the loading control. (e) Luciferase reporter analyses of wild-type *FSCN1* promoter ("Wild type") and mutant *FSCN1* promoter ("Point mutant") in LYAR knockdown HCT15 cells. Results are shown as the mean \pm standard deviation ($n = 3$). ** $p < 0.01$ compared with the scrambled shRNA control.

expression of *FSCN1*, one of the candidate genes, was consistently lower in LYAR-KD cells compared to the control (Figure 3(c)). Downstream involvement of *FSCN1* in LYAR-regulated CRC would be a novel finding; we therefore conducted further experiments to verify this relationship between LYAR and *FSCN1*. We detected *FSCN1* expression

after LYAR knockdown by siRNA in all three cell lines and found that *FSCN1* was only downregulated in HCT15 (Figure 3(d) and Figure S5). We therefore performed the subsequent experiments only in HCT15 cells. Together, these results indicated that *FSCN1* is a potential target of LYAR in CRC cells.

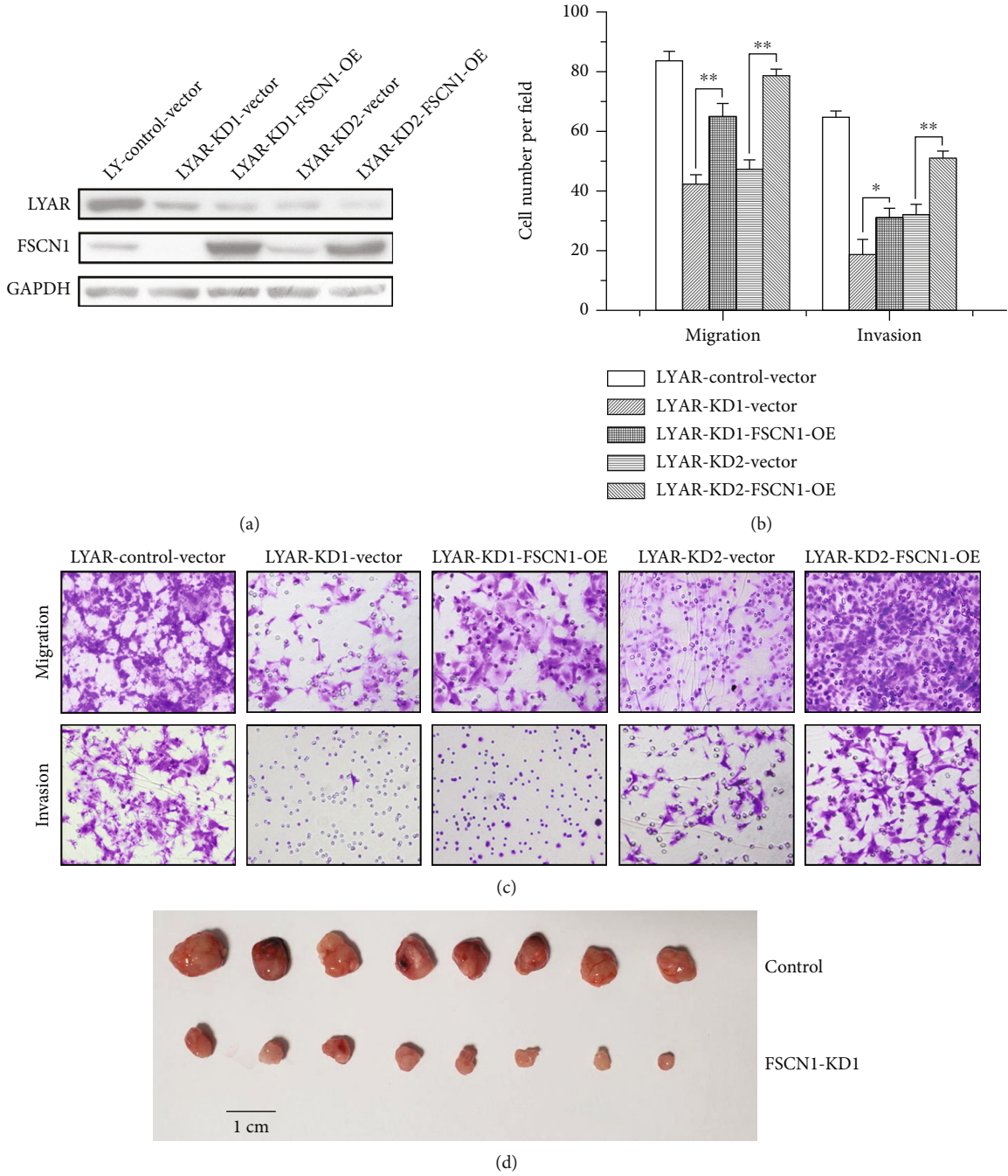


FIGURE 5: Continued.

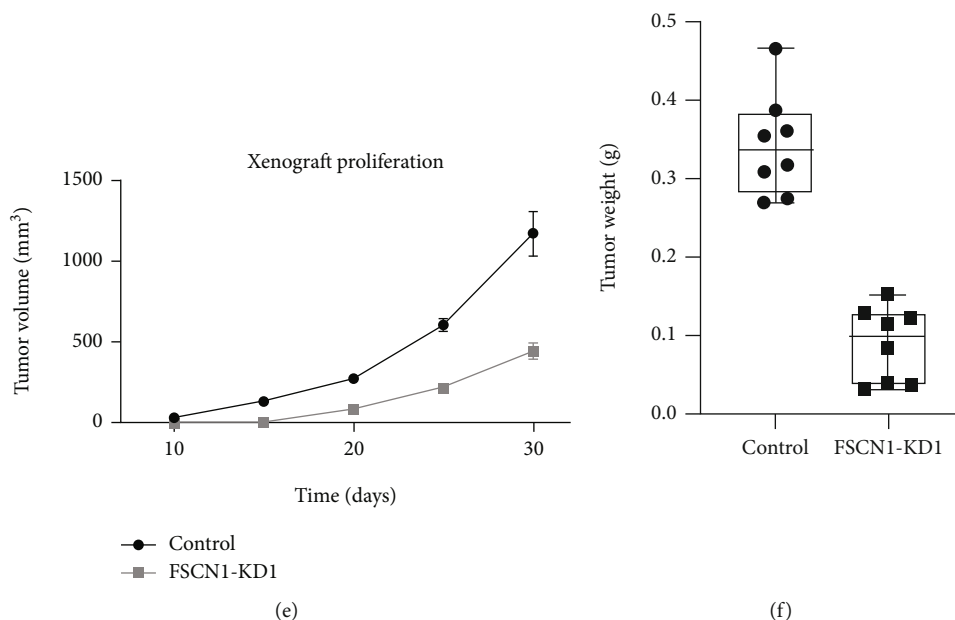


FIGURE 5: *FSCN1* overexpression restores the metastatic potential of *LYAR* knockdown cells. (a) Western blot assay showing *LYAR* and *FSCN1* protein expression in *LYAR* knockdown (KD) HCT15 cells with and without *FSCN1* overexpression (OE). GAPDH served as the loading control. (b) Representative photos of haptotactic migration assay and matrigel chemoinvasion assay using *LYAR* knockdown HCT15 cells with and without *FSCN1* overexpression. Original magnification, 200x. (c) Results of the migration and invasion assays shown in (b). Data are shown as the mean \pm standard deviation ($n = 3$). $**p < 0.01$ and $*p < 0.05$ compared with the empty vector control. (d) Xenografted tumors of negative control (NC) cells and stable *FSCN1*-KD HCT15 cells ($n = 8$). (e) Tumor volumes over time. (f) Xenografted tumors were resected and weighed at the end of the experiment. Results are shown as the mean \pm standard deviation ($n = 8$). $*p < 0.05$, $**p < 0.01$, and $***p < 0.001$. OE: stable *FSCN1* overexpression in *LYAR* knockdown (KD) HCT15 cells.

3.3. *LYAR* Binds to the *FSCN1* Promoter in CRC Cells. We identified a consensus DNA-binding motif of *LYAR* (GGTTAG) at -237 bp upstream of the *FSCN1* gene transcriptional start site (Figure 4(a) and Table S2). Chromatin immunoprecipitation (ChIP) analysis spanning the promoter of the *FSCN1* gene was performed to determine if *LYAR* binds to the *FSCN1* promoter and regulates its expression. *LYAR* indeed bound to the *FSCN1* promoter region between -337 and -183 bp in HCT15 cells (Figure 4(b)). When *LYAR* was knocked down in HCT15 cells with shRNAs, *LYAR* enrichment on the *FSCN1* promoter was significantly reduced (Figure 4(c)). Furthermore, a luciferase reporter assay showed that the extent of *LYAR* binding to the *FSCN1* promoter corresponded to changes in *LYAR* expression in HCT15 cells transfected with a wild-type *FSCN1* promoter-driven luciferase construct (Figures 4(d) and 4(e)). Mutating the *LYAR* binding motif from GGTTAG to GACTAG abolished corresponding *FSCN1* promoter activity changes (Figures 4(d) and 4(e)). In summary, these results demonstrated that *LYAR* directly regulates *FSCN1* gene expression and that the *LYAR*-binding motif (GGTTAG) in the promoter of *FSCN1* plays a critical role in *LYAR*-mediated transcriptional activation of *FSCN1*.

3.4. Ectopic Expression of *FSCN1* Restores Migration and Invasion Potential of *LYAR*-KD Cells. *FSCN1* has been reported to increase CRC migration and invasion in cell cultures and cause cell dissemination and metastasis *in vivo* [27]. In this study, we found that knockdown of

LYAR by shRNAs in HCT15 cells led to downregulation of *FSCN1* (Figures 3(c) and 3(d)) and that the cell migration and invasion potential were correspondingly decreased (Figures 2(c) and S4). To investigate the role of *FSCN1* in *LYAR*-promoted CRC cell migration and invasion, rescue experiments were performed in *LYAR*-KD cells in which *FSCN1* was overexpressed by a stably transfected *FSCN1*-coding sequence. Overexpression of *FSCN1* and knockdown of *LYAR* were confirmed by Western blot in HCT15 cells (Figure 5(a)). Compared with the control *LYAR*-KD cells (*LYAR*-KD-Vector), the migration and invasion potential of the HCT15 cells with *FSCN1* overexpression was significantly increased (Figures 5(b) and 5(c)), indicating that exogenous expression of *FSCN1* partially restored cell migration and invasion potential of *LYAR*-KD cells. To test this effect *in vivo*, stable *FSCN1*-KD or control HCT15 cells were subcutaneously adoptively transferred to nude mice. Xenografts in the *FSCN1*-KD group were significantly inhibited compared to those in the control group (Figures 5(d)–5(f)). In summary, these results indicated that *FSCN1* plays a key role in mediating *LYAR*-promoted CRC cell migration and invasion.

3.5. Reduction of *FSCN1* Expression in CRC Cells Inhibits the Expression of Some Key Enzymes in Fatty Acid Metabolism. To clarify the mechanism of *FSCN1* in promoting tumor invasion and metastasis, RNA-Seq was used to search for potential *FSCN1* targets and signaling pathways. In the *FSCN1*-KD line, metabolic pathways, including lipid

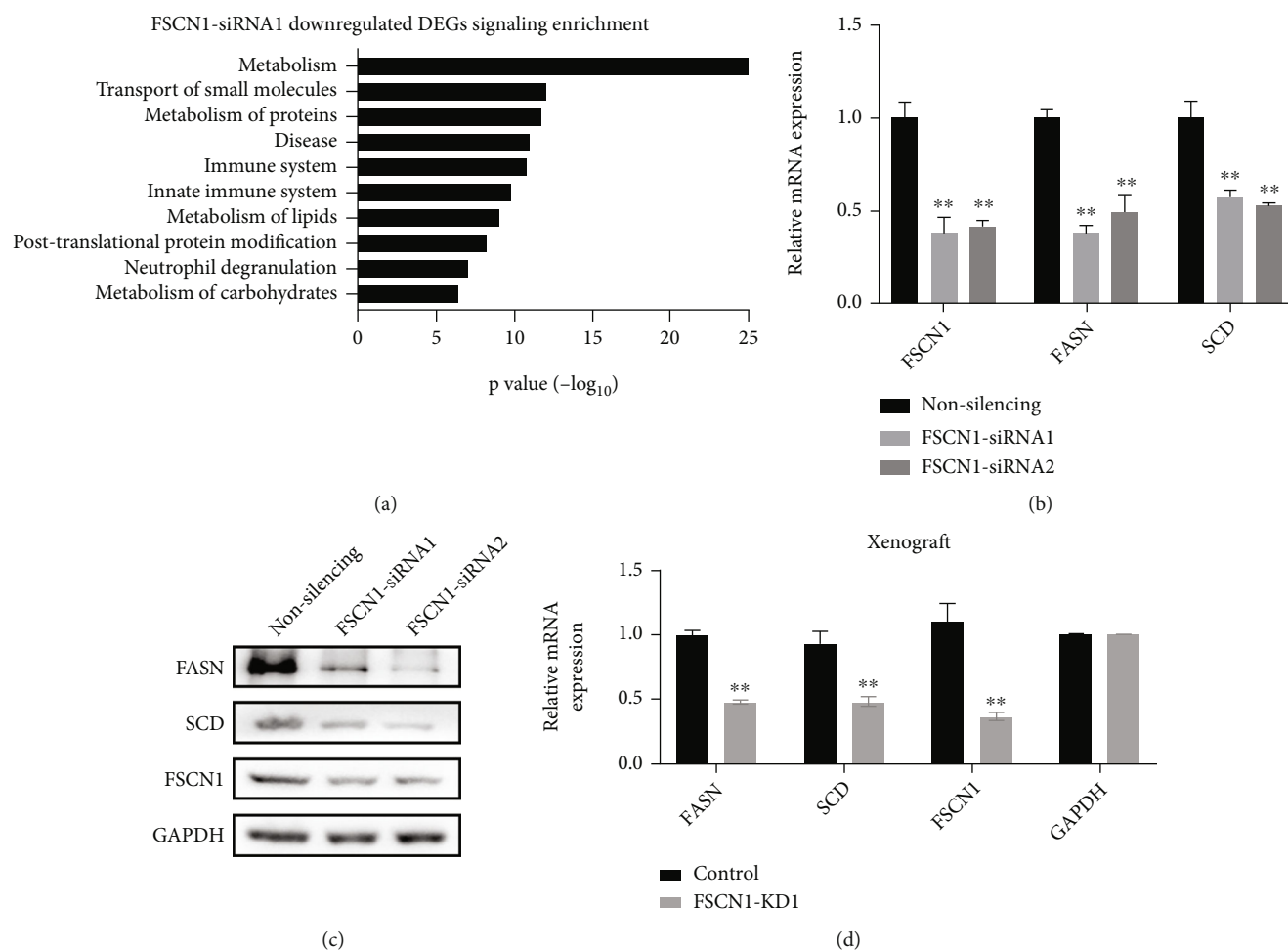


FIGURE 6: Reduction of *FSCN1* expression in CRC cells inhibits the expression of some key enzymes in fatty acid metabolism. (a) Downregulated genes (fold change > 2) were enriched in several pathways (based on the Reactome pathway database). (b) Quantitative real-time PCR analysis of *FSCN1*, *FASN*, and *SCD* from *FSCN1* knockdown or control HCT15 cells. Results are shown as the mean \pm standard deviation ($n = 3$). ** $p < 0.01$ compared with the control. (c) Western blot assay showing *FSCN1*, *FASN*, and *SCD* protein expression in *FSCN1* knockdown HCT15 cells. GAPDH served as the loading control. (d) Quantitative real-time PCR analysis of *FASN*, *SCD*, and *FSCN1* in *FSCN1* knockdown or control HCT15 cells from xenograft. ** $p < 0.01$ compared with the control.

metabolism, were enriched (Figure 6(a)). Because our previous analysis showed that *LYAR* knockdown caused a reduction in cholesterol homeostasis, which is also a lipid metabolism pathway (Figure 3(b)), we further investigated the influence of *FSCN1* inhibition on key enzymes in lipid metabolism. Among the lipid metabolism-related genes, the expression of fatty acid synthase (*FASN*) and stearoyl-CoA desaturase (*SCD*) were consistently decreased in *FSCN1*-KD HCT15 cells compared to the control at both the mRNA (Figure 6(b)) and protein (Figure 6(c)) levels. It was previously reported that *de novo* synthesis of palmitic acid from acetyl-CoA is mainly catalyzed by *FASN*; moreover, saturated fatty acids (SFAs) are converted into mono-unsaturated fatty acids (MUFAs) by *SCD*, and their chains are elongated by elongases [28]. These data suggest that *FSCN1* positively regulates fatty acid metabolism.

In xenograft samples, *FASN* and *SCD* were also downregulated in the *FSCN1*-KD line (Figure 6(d)). Intriguingly, the analysis of TCGA CRC data revealed that the expression levels of *LYAR*, *FSCN1*, *FASN*, and *SCD* in CRC tissues were

all higher than those in normal tissues (Figure S6). This suggests that *LYAR* may promote CRC progression by upregulating *FSCN1* expression and subsequent fatty acid metabolism, which is logically consistent with the results of our *in vitro* experiments (Figures 6(b)–6(d)). In conclusion, our data demonstrated the presence of a *LYAR/FSCN1*/fatty acid metabolism axis which promoted the growth of CRC tumors *in vivo*.

4. Discussion

The formation of metastasis is a complex, multistep process, and the molecular mechanisms of CRC metastasis are still not fully understood. In recent years, some studies have found that *LYAR* plays an important role in different biological processes, such as RNA synthesis and the development of erythroid cells [14–18, 29, 30]. *LYAR* may be involved in the *MYCN* signaling pathway in the development of medulloblastoma [31] and induces neuroblastoma cell proliferation and survival [32], and *LYAR* together with other

five genes (*PDIA3*, *NOPI4*, *NCALD*, *MTSS1*, and *CYP11B1*) can be used as potential prognostic biomarkers for curative and postoperative supportive therapies for ovarian cancer [33]. However, aside from these, there have been no other reports on the function of LYAR in cancer.

We previously found that LYAR was expressed at a higher level in metastatic CRC tissues and that it promotes tumor cell migration and invasion by upregulating *LGALS1* expression in CRC cell lines [20]. However, that study lacked *in vivo* experiments; the potential of LYAR to promote metastasis could not be verified, and retrospective analysis could not be conducted on the survival of clinical CRC patients to hypothesize whether LYAR was an independent prognostic factor. In addition, the heterogeneity of solid tumors makes it unlikely that upregulating the expression of *LGALS1* is the only molecular mechanism by which LYAR promotes CRC migration and invasion among all colorectal cancers with high LYAR expression.

In this study, we used large-scale immunohistochemical tissue microarrays and found that LYAR is highly expressed in CRC tissues. This high expression is positively correlated with the metastatic rate of CRC and is significantly correlated with poor CRC prognosis. Moreover, we performed a genome-wide expression profile analysis to further study heterogeneity in molecular mechanisms through which LYAR participates in the progression of colorectal cancer, demonstrating that LYAR plays a role in the promotion of CRC invasion and metastasis by upregulating *FSCN1* expression. However, we detected the expression of *FSCN1* after LYAR siRNA knockdown in three different cell lines and found that *FSCN1* was only downregulated in HCT15. This suggested that LYAR regulates *FSCN1* expression in only a subset of colorectal cancers. This phenomenon may be due to differences in race, gender, and age of the patients from whose tissue different colorectal cancer cell lines are derived; these can lead to differences in molecular features between cell lines. This result again illustrates that solid tumors exhibit significant heterogeneity.

FSCN1 has recently been shown to promote cancer cell migration and invasion through its role in formation of cellular protrusions such as filopodia and invadopodia [34]. Forced expression of *FSCN1* in CRC cells increased their migration and invasion *in vitro* and caused cell dissemination and metastasis *in vivo* [27]. Another recent study showed that imipramine, a novel *FSCN1* inhibitor, has been confirmed to have significant antitumor effects both *in vivo* and *in vitro*, which lays the foundation for molecular targeted therapy of serrated adenocarcinoma (SAC) and other *FSCN1*-overexpressing tumors [35]. In this study, we revealed that LYAR positively regulates *FSCN1* expression. We also found that LYAR knockdown in CRC cells led to the reduction of *FSCN1* levels and inhibited metastasis to the lungs and liver in NOD/SCID mice. This is consistent with the report that forced expression of *FSCN1* in CRC cells caused cell dissemination and metastasis *in vivo*.

There is previous evidence in the literature of *FSCN1* involvement in tumor metabolism. In lung cancer, *FSCN1* promotes cancer growth and metastasis by enhancing gly-

colysis and *PFKFB3* expression through *YAP1* activation [36]. In the context of *PIK3CA* mutation or amplification, high expression of *FSCN1* is associated with poor prognosis and radiotherapy response in cancer patients; mutant *PIK3CA* (E542K and E545K) can enhance glucose metabolism and cell proliferation in cancer cells [37, 38]. In the present study, separate from glucose metabolism, we demonstrated that *FSCN1* was related to lipid metabolism in CRC. *FSCN1* knockdown reduced the expression of *FASN* and *SCD*, which are key genes in *de novo* fatty acid synthesis, suggesting that *FSCN1* promoted CRC by affecting lipid metabolism.

This regulatory action of *FSCN1* may be because CRC is closely related to obesity and lipid metabolism [39, 40]. Fatty acids are indispensable for the biosynthesis of most lipids, such as membrane lipids and lipid signaling molecules, in addition to acting as substrates for energy production [41]. *De novo* synthesis of palmitic acid from acetyl-CoA (acetyl-coenzyme A) is mainly catalyzed by fatty acid synthase (*FASN*). SFAs are converted into MUFAs by stearoyl-CoA desaturase 1 (*SCD*), and their chains are elongated by elongases [28]. A high-fat diet increases palmitic acid levels, which in turn increase β 2AR expressions in a Sp-1 dependent manner. Subsequently, the cAMP/PKA axis is activated and hormone sensitive lipase (HSL) is phosphorylated at S552 to increase energy production, which promotes CRC growth [42]. In addition, there may be another *FSCN1*-lipid metabolism axis independent of LYAR, which would require future studies to confirm.

In summary, we demonstrated that *FSCN1* is a direct target of LYAR. A novel pathway for function of the transcription factor LYAR in CRC has also been revealed: LYAR promotes tumor migration and invasion by upregulating *FSCN1* expression, which in turn positively regulates fatty acid metabolism. These findings suggest that LYAR could be used as a prognostic and therapeutic candidate target for the prevention and treatment of CRC.

Data Availability

The data generated or analyzed during the current study are available from the corresponding author on reasonable request.

Ethical Approval

All research involving human CRC tissues was approved by the Ethics Committee of Bengbu Medical College and was in accordance with the principles of the Declaration of Helsinki. All animal studies were approved by the ethical regulations of Institutional Animal Care and Use Committee (IACUC) of Suzhou University.

Conflicts of Interest

The authors declare no conflict of interest.

Authors' Contributions

S. Ma, X.Y. Song, and Y.P. Wu conceived the idea; Y. Zhou performed the animal experiments; H.Y. Gao and Y.P. Wu performed development of methodology and acquisition of data; Q.Y. Cheng and S.K. Jian finished acquisition of data and interpretation of data; Q. Ding and W. Gu finished acquisition of data; Y.X. Yao and X.H. Tong conducted the statistical analysis; J. Ma, W.J. Wu, and Y.Y. Li conducted the bioinformatics analyses; Y.P. Wu, H.Y. Gao, Y.J. Wang, X.Y. Song, and S. Ma wrote the manuscript and all of the authors read and reviewed and approved the manuscript. Yupeng Wu, Yu Zhou, and Haiying Gao contributed equally to this work.

Acknowledgments

This work was supported by the Natural Science Research Project of Anhui Educational Committee (KJ2019A0318), Funds for the Construction of Medical Technology Disciplines of Bengbu Medical College, Science Research Project of Bengbu Medical College (BYKF1804), and the Hefei National Laboratory for Physical Sciences at the Microscale (KF2020011). We are grateful to members of Dr. Wang Mingrong Laboratories (State Key Laboratory of Molecular Oncology, Cancer Hospital and Institute, Chinese Academy of Medical Sciences, Peking Union Medical College, Beijing, China) and Dr. Zhao Quan Laboratories (State Key Laboratory of Pharmaceutical Biotechnology, School of Life Sciences, Nanjing University, Nanjing, China) for technical assistance and helpful discussions.

Supplementary Materials

Figure S1: Overall survival curve of those with colorectal cancer. Data were obtained from TCGA database and analyzed to generate Kaplan-Meier curves, which show a correlation between patients with tumors expressing low levels of LYAR and higher survival rates. Figure S2: LYAR expression in stable LYAR knockdown HCT15 cells. (a) RT-qPCR analysis of LYAR gene expression normalized to GAPDH gene expression in stable LYAR knockdown HCT15 cells. $**p < 0.01$ compared with the scrambled control. (b) Western blot assay showing LYAR protein expression in stable LYAR knockdown HCT15 cells. GAPDH served as the loading control. Figure S3: Detection of tumor cell phenotype in transient LYAR knockdown HCT15 cells. LYAR knockdown had no effect on cell proliferation (a), cell adhesion (b), cell cycle (c), apoptosis (d), or colony formation (e) of HCT15 cells. Parental refers to the control, nonsilencing refers to cells transfected with a nonspecific siRNA, and LYAR-siRNA1 and LYAR-siRNA2 refer to cells transfected with LYAR-specific siRNA1 and LYAR-specific siRNA2, respectively. Figure S4: Detection of migration and invasion in stable LYAR knockdown HCT15 cells. (a) Representative photos of haptotactic migration assay and matrigel chemoinvasion assay using stable LYAR knockdown HCT15 cells. Original magnification, 200x. (b) Results of migration and invasion assays. Data shown are the mean \pm standard

deviation ($n = 3$). $**p < 0.01$ compared to the scrambled control. Figure S5: Western blot assay showing FSCN1 expression after LYAR knockdown by siRNA. (a) LYAR and FSCN1 expression after LYAR knockdown in HCT8 cells. (b) LYAR and FSCN1 expression after LYAR knockdown in HCT116 cells. KD1 and KD2 refer to the stable LYAR knockdown lines LYAR-siRNA1 and LYAR-siRNA2, respectively. Figure S6: Expression of LYAR and downstream genes in colorectal cancer. The expression profiles of human colorectal cancer and normal colon tissue were obtained from TCGA and GTEx databases, respectively. The data show differential expression of LYAR (a), FSCN1 (b), FASN (c), and SCD (d) in colorectal cancer tissues compared to adjacent normal tissues. $***p < 0.001$ and $****p < 0.0001$. Table S1: The relationship between LYAR protein expression and clinicopathological features in CRC patients. Table S2: ChIP primer sequences for the FSCN1 promoter. (*Supplementary Materials*)

References

- [1] F. Bray, J. Ferlay, I. Soerjomataram, R. L. Siegel, L. A. Torre, and A. Jemal, "Global cancer statistics 2018: GLOBOCAN estimates of incidence and mortality worldwide for 36 cancers in 185 countries," *CA: a Cancer Journal for Clinicians*, vol. 68, no. 6, pp. 394–424, 2018.
- [2] E. J. Kuipers, W. M. Grady, D. Lieberman et al., "Colorectal cancer," *Nature Reviews. Disease Primers*, vol. 1, no. 1, p. 15065, 2015.
- [3] R. L. Siegel, K. D. Miller, and A. Jemal, "Cancer statistics, 2020," *CA: a Cancer Journal for Clinicians*, vol. 70, no. 1, pp. 7–30, 2020.
- [4] R. M. Lee, K. Cardona, and M. C. Russell, "Historical perspective: two decades of progress in treating metastatic colorectal cancer," *Journal of Surgical Oncology*, vol. 119, no. 5, pp. 549–563, 2019.
- [5] M. Tsitskari, D. Filippidis, and C. Kostantinos, "The role of interventional oncology in the treatment of colorectal cancer liver metastases," *Annals of Gastroenterology*, vol. 32, no. 2, pp. 147–155, 2019.
- [6] X. Guan, "Cancer metastases: challenges and opportunities," *Acta Pharmaceutica Sinica B*, vol. 5, no. 5, pp. 402–418, 2015.
- [7] P. S. Steeg, "Tumor metastasis: mechanistic insights and clinical challenges," *Nature Medicine*, vol. 12, no. 8, pp. 895–904, 2006.
- [8] D. Hanahan and R. A. Weinberg, "The hallmarks of cancer," *Cell*, vol. 100, no. 1, pp. 57–70, 2000.
- [9] on behalf of the Cancer Research UK and Cancer Therapeutics CRC Australia Metastasis Working Group, R. L. Anderson, T. Balasas et al., "A framework for the development of effective anti-metastatic agents," *Nature Reviews. Clinical Oncology*, vol. 16, no. 3, pp. 185–204, 2019.
- [10] C. L. Chaffer and R. A. Weinberg, "A perspective on cancer cell metastasis," *Science*, vol. 331, no. 6024, pp. 1559–1564, 2011.
- [11] S. Y. Guraya, "Pattern, stage, and time of recurrent colorectal cancer after curative surgery," *Clinical Colorectal Cancer*, vol. 18, no. 2, pp. e223–e228, 2019.
- [12] L. Su, R. J. Hershberger, and I. L. Weissman, "LYAR, a novel nucleolar protein with zinc finger DNA-binding motifs, is

- involved in cell growth regulation," *Genes & Development*, vol. 7, no. 5, pp. 735–748, 1993.
- [13] H. Li, B. Wang, A. Yang et al., "Ly-1 antibody reactive clone is an important nucleolar protein for control of self-renewal and differentiation in embryonic stem cells," *Stem Cells*, vol. 27, no. 6, pp. 1244–1254, 2009.
- [14] N. Luna-Pelaez and M. Garcia-Dominguez, "Lyar-mediated recruitment of Brd2 to the chromatin attenuates *_Nanog_* downregulation following induction of differentiation," *Journal of Molecular Biology*, vol. 430, no. 8, pp. 1084–1097, 2018.
- [15] K. Izumikawa, H. Ishikawa, H. Yoshikawa et al., "LYAR potentiates rRNA synthesis by recruiting BRD2/4 and the MYST-type acetyltransferase KAT7 to rDNA," *Nucleic Acids Research*, vol. 47, no. 19, pp. 10357–10372, 2019.
- [16] K. Yonezawa, Y. Sugihara, K. Oshima, T. Matsuda, and D. Nadano, "Lyar, a cell growth-regulating zinc finger protein, was identified to be associated with cytoplasmic ribosomes in male germ and cancer cells," *Molecular and Cellular Biochemistry*, vol. 395, no. 1–2, pp. 221–229, 2014.
- [17] D. Datta, K. Anbarasu, S. Rajabather, R. S. Priya, P. Desai, and S. Mahalingam, "Nucleolar GTP-binding protein-1 (NGP-1) promotes G₁ to S phase transition by activating cyclin-dependent kinase inhibitor p21^{Cip1/Waf1}," *The Journal of Biological Chemistry*, vol. 290, no. 35, pp. 21536–21552, 2015.
- [18] C. Yang, X. Liu, T. Cheng et al., "LYAR suppresses beta interferon induction by targeting phosphorylated interferon regulatory factor 3," *Journal of virology*, vol. 93, no. 21, 2019.
- [19] J. Ju, Y. Wang, R. Liu et al., "Human fetal globin gene expression is regulated by LYAR," *Nucleic Acids Research*, vol. 42, no. 15, pp. 9740–9752, 2014.
- [20] Y. Wu, M. Liu, Z. Li et al., "LYAR promotes colorectal cancer cell mobility by activating galectin-1 expression," *Oncotarget*, vol. 6, no. 32, pp. 32890–32901, 2015.
- [21] L. Astorgues-Xerri, M. E. Riveiro, A. Tijeras-Raballand et al., "Unraveling galectin-1 as a novel therapeutic target for cancer," *Cancer Treatment Reviews*, vol. 40, no. 2, pp. 307–319, 2014.
- [22] J. C. Adams, "Roles of fascin in cell adhesion and motility," *Current Opinion in Cell Biology*, vol. 16, no. 5, pp. 590–596, 2004.
- [23] A. Jayo and M. Parsons, "Fascin: a key regulator of cytoskeletal dynamics," *The International Journal of Biochemistry & Cell Biology*, vol. 42, no. 10, pp. 1614–1617, 2010.
- [24] H. Liu, J. Cui, Y. Zhang et al., "Mass spectrometry-based proteomic analysis of FSCN1-interacting proteins in laryngeal squamous cell carcinoma cells," *IUBMB Life*, vol. 71, no. 11, pp. 1771–1784, 2019.
- [25] Z. Xu, X. Gao, Y. He et al., "Synergistic effect of SRY and its direct target, WDR5, on Sox9 expression," *PLoS One*, vol. 7, no. 4, article e34327, 2012.
- [26] Q. Zhao, G. Rank, Y. T. Tan et al., "PRMT5-mediated methylation of histone H4R3 recruits DNMT3A, coupling histone and DNA methylation in gene silencing," *Nature Structural & Molecular Biology*, vol. 16, no. 3, pp. 304–311, 2009.
- [27] D. Vignjevic, M. Schoumacher, N. Gavert et al., "Fascin, a novel target of beta-catenin-TCF signaling, is expressed at the invasive front of human colon cancer," *Cancer Research*, vol. 67, no. 14, pp. 6844–6853, 2007.
- [28] E. Currie, A. Schulze, R. Zechner, T. C. Walther, and R. V. Farese Jr., "Cellular fatty acid metabolism and cancer," *Cell Metabolism*, vol. 18, no. 2, pp. 153–161, 2013.
- [29] G. Wang, C. M. Fulkerson, R. Malek, S. Ghassemifar, P. W. Snyder, and S. M. Mendrysa, "Mutations in Lyar and p53 are synergistically lethal in female mice," *Part A, Clinical and molecular teratology*, vol. 94, no. 9, pp. 729–737, 2012.
- [30] D. A. Abetov, V. S. Kiyani, A. A. Zhylykabayev et al., "Editors' pick: native mammalian preribosomal complexes," *The Journal of Biological Chemistry*, vol. 294, no. 28, pp. 10746–10757, 2019.
- [31] F. J. Swartling, M. R. Grimmer, C. S. Hackett et al., "Pleiotropic role for MYCN in medulloblastoma," *Genes & Development*, vol. 24, no. 10, pp. 1059–1072, 2010.
- [32] Y. Sun, B. Atmadibrata, D. Yu et al., "Upregulation of LYAR induces neuroblastoma cell proliferation and survival," *Cell Death and Differentiation*, vol. 24, no. 9, pp. 1645–1654, 2017.
- [33] H. S. Isaksson, B. Sorbe, and T. K. Nilsson, "Whole genome expression profiling of blood cells in ovarian cancer patients -prognostic impact of the CYP1B1, MTSS1, NCALD, and NOP14," *Oncotarget*, vol. 5, no. 12, pp. 4040–4049, 2014.
- [34] X. Sui, J. Zhu, H. Tang et al., "p53 controls colorectal cancer cell invasion by inhibiting the NF- κ B-mediated activation of Fascin," *Oncotarget*, vol. 6, no. 26, pp. 22869–22879, 2015.
- [35] B. Alburquerque-González, M. Bernabé-García, S. Montoro-García et al., "New role of the antidepressant imipramine as a Fascin1 inhibitor in colorectal cancer cells," *Experimental & Molecular Medicine*, vol. 52, no. 2, pp. 281–292, 2020.
- [36] S. Lin, Y. Li, D. Wang et al., "Fascin promotes lung cancer growth and metastasis by enhancing glycolysis and PFKFB3 expression," *Cancer Letters*, vol. 518, pp. 230–242, 2021.
- [37] S. Li, X. T. Huang, M. Y. Wang et al., "FSCN1 promotes radiation resistance in patients with PIK3CA gene alteration," *Frontiers in Oncology*, vol. 11, article 653005, 2021.
- [38] W. Jiang, T. He, S. Liu et al., "The PIK3CA E542K and E545K mutations promote glycolysis and proliferation via induction of the β -catenin/SIRT3 signaling pathway in cervical cancer," *Journal of Hematology & Oncology*, vol. 11, no. 1, p. 139, 2018.
- [39] W. A. Keshk, D. H. Zineldeen, R. E. Wasfy, and O. H. el-Khadrawy, "Fatty acid synthase/oxidized low-density lipoprotein as metabolic oncogenes linking obesity to colon cancer via NF-kappa B in Egyptians," *Medical Oncology*, vol. 31, no. 10, p. 192, 2014.
- [40] X. Pu and D. Chen, "Targeting adipokines in obesity-related tumors," *Frontiers in Oncology*, vol. 11, article 685923, 2021.
- [41] X. Luo, C. Cheng, Z. Tan et al., "Emerging roles of lipid metabolism in cancer metastasis," *Molecular Cancer*, vol. 16, no. 1, p. 76, 2017.
- [42] S. Fatima, X. Hu, C. Huang et al., "High-fat diet feeding and palmitic acid increase CRC growth in β 2AR- dependent manner," *Cell Death & Disease*, vol. 10, no. 10, p. 711, 2019.